

Integration of Flexible and Microscale Organic Nonvolatile Resistive Memory Devices Using Orthogonal Photolithography

Younggul Song¹, Jingon Jang¹, Daekyoung Yoo¹, Seok-Heon Jung², Hyunhak Jeong¹,
Seunghun Hong¹, Jin-Kyun Lee², and Takhee Lee^{1,*}

¹Department of Physics and Astronomy, and Institute of Applied Physics, Seoul National University, Seoul 151-747, Korea

²Department of Polymer Science and Engineering, Inha University, Incheon 402-751, Korea

We present the integration of flexible and microscale organic nonvolatile resistive memory devices fabricated in a cross-bar array structure on plastic substrates. This microscale integration was made via orthogonal photolithography method using fluorinated photoresist and solvents and was achieved without causing damage to the underlying organic memory materials. Our flexible microscale organic devices exhibited high ON/OFF ratio ($I_{ON}/I_{OFF} > 10^4$) under bending conditions. In addition, the ON and OFF states of our flexible and microscale memory devices were maintained for 10,000 seconds without any serious degradation.

Keywords: Organic Electronics, Organic Memory, Nonvolatile Resistive Memory, Cross-Bar Architecture, Microlithography.

1. INTRODUCTION

Organic electronic devices have recently received noteworthy attention for their various advantages, including large area processing capabilities, printing process, low manufacturing cost, and flexibility.^{1–6} Due to these advantages, researchers have investigated the variety of possible applications for these new devices, such as organic field effect transistors, organic light-emitting diodes, organic photovoltaic cells, organic sensors, and organic memories.^{3–9} Specifically, organic nonvolatile memory in which confined nanoparticles are embedded in insulating polymer matrix is considered to be a promising candidate for information storage devices because of its ease of fabrication, nice performance, durability, and flexibility.^{9–16} Organic memory devices have usually been fabricated in a cross-bar structure, which can achieve high integration of memory cells.^{10–16}

Recently, fabrication of organic memory devices on the flexible substrate such as polyethylene naphthalate (PEN) or poly(ethylene terephthalate) (PET) have been studied.^{16–21} However, the integration of the flexible

organic memory devices has not been beyond 64 bits and the individual cell size of cross-bar structured organic memory devices has usually been limited to several hundreds of microns (μm) using shadow mask method.^{16–21} Because of the chemical incompatibility between organic electronic materials and organic solvents (such as developer and acetone) used for the conventional photolithographic patterning, the standard photolithography method cannot be applied to scale down the organic memory devices. Other substitutive methods for fabrication of microscale organic memory devices (e.g., nanowire pattern transfer, the direct metal-transfer method, and a method using photo cross-linkable organic memory)^{22–24} have complicated and unpractical processes, which obstruct the fabrication of microscale integration of organic devices on a flexible substrate. However some groups, including us, have demonstrated a chemically non-damaging orthogonal photolithographic method which protects the underlying polymer organic films from the action of lithographic chemicals.^{25–29} The solution is to use fluorinated photoresist (such as semiperfluoroalkyl resorcinarene) and solvents (such as hydrofluoroethers) which are miscible to each other and orthogonal to most organic materials and flexible substrates. These materials allow organic

*Author to whom correspondence should be addressed.

electronic devices to be fabricated at the microscale using the photolithography process.^{25, 27, 29}

In this study, we demonstrate the integration of flexible and microscale organic nonvolatile resistive memory devices with 4,096 bit (64×64) organic memory cells in $1.9 \times 1.9 \text{ mm}^2$ with cross-point architecture on a plastic substrate. The fabrication of the devices was possible by using orthogonal photolithography process using fluorinated resist and solvents. And we studied the electrical characteristics of our flexible organic memory devices under different bending conditions (bending radius of 10 mm and 5 mm).

2. EXPERIMENTAL DETAILS

Figure 1 shows the schematics of fabrication process and optical image of the flexible and microscale organic memory devices on a plastic substrate. First, a PET substrate was prepared and ultrasonically cleaned using acetone, isopropanol, and de-ionized water. Then, Al (20 nm)/Au (15 nm)/Ti (5 nm) were deposited for bottom electrodes on the PET substrate. Here, Au/Ti bilayer (Ti as an adhesion layer and Au as a buffer layer) reduces the oxidation of the bottom Al electrode caused by the PET substrate material.¹⁹ The bottom electrodes with a width of $10 \mu\text{m}$ were patterned by the standard photolithography and lift-off process. The patterned bottom electrodes on the PET substrate were then exposed to UV-ozone for 10 min. In this study, a composite of PI (polyimide) and PCBM (6-phenyl-C61 butyric acid methyl ester) was used as the active memory layer due to its mechanical robustness and thermal stability.^{13, 17, 19, 22} For the active memory material (PI:PCBM), 2 ml of BPDA-PPD (3,4,3',4'-biphenyltetracarboxylic dianhydride-*p*-phenylene diamine) solution (10 wt% in NMP (N-methyl-2-pyrrolidone)) and 0.3 ml of PCBM solution (0.5 wt% in NMP) were mixed and then diluted with 11.3 ml of NMP to control the active

layer thickness. Then, the prepared memory solution was spin coated onto the substrate at 1500 rpm for 35 s, followed by soft-baking on a hot plate at $120 \text{ }^\circ\text{C}$ for 5 min. After the PI:PCBM film on the Al electrode pads was removed using cotton swab wet with methanol, the remaining PI:PCBM layer on the substrate was hard-baked on a hot plate at $200 \text{ }^\circ\text{C}$ for 2 hours (see Fig. 1(a)).

For the orthogonal photolithography to fabricate microscale organic memory devices, we used R_F -Calix-tBoc (semi-perfluoroalkyl resorcinarene) as photoresist and HFE-7200 (3-ethoxy-1,1,1,2,3,4,4,5,5,6,6,6-dodecafluoro-2trifluoromethylhexane) as developer. These photoresist and solvent are highly fluorinated materials, which are miscible to each other and orthogonal to most organic electronic materials including PI:PCBM.²⁵⁻²⁸ To prepare the fluorinated photoresist solution, 10 wt% of R_F -Calix-tBoc powder and 0.5 wt% of photoacid generator (N-nonafluorobutanesulfonyloxy-1,8-naphthalimide) were dissolved into a mixed solvent (HFE-7500 (3-ethoxy-1,1,1,2,3,4,4,5,5,6,6,6-dodecafluoro-2trifluoromethylhexane): PGMEA (propylene glycol methyl ether acetate) = 4:1 weight ratio), and the solution was filtered through a $0.20\text{-}\mu\text{m}$ nylon syringe filter. Then the prepared fluorinated photoresist solution was spin coated at 1500 rpm for 50 s, followed by baking process at $75 \text{ }^\circ\text{C}$ for 3 min under yellow light (Fig. 1(b)). Subsequently, the coated photoresist film was exposed under UV light through a photomask with $10 \mu\text{m}$ lines orthogonal to the patterned Al/Au/Ti bottom electrode lines (Fig. 1(c)). After post-exposure baking at $75 \text{ }^\circ\text{C}$ for 3 min, the photoresist film was developed by HFE-7200 and dried with N_2 gas (Fig. 1(d)). To make the top electrodes, a 30 nm-thick Au layer was deposited on the developed samples. Finally, for the flexible and microscale organic memory array devices, the sample was lifted off in an ethanol (5 vol%)-HFE-7200 (95 vol%) mixture to leave patterned Au electrodes on top of the PI:PCBM film (Fig. 1(e)).

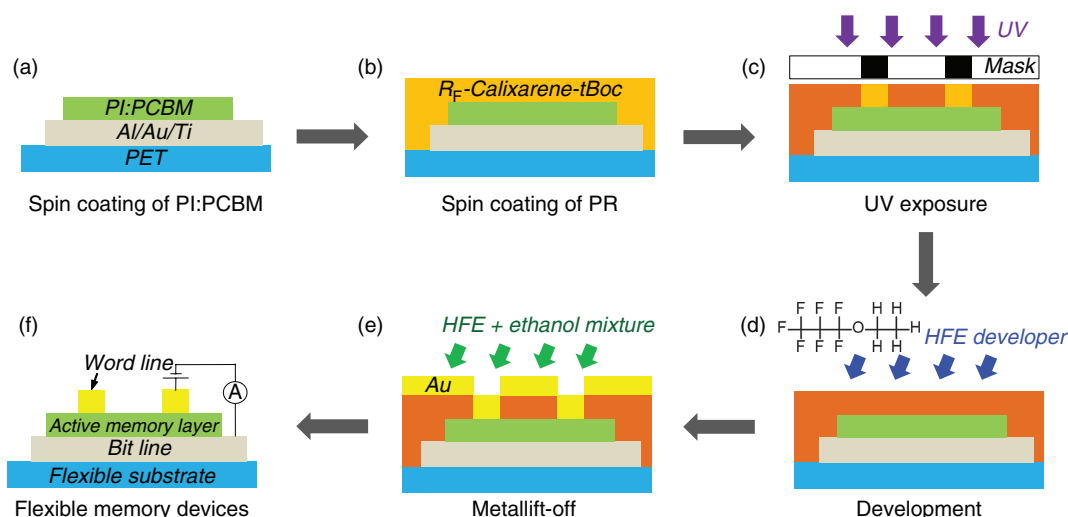


Figure 1. The schematics illustrating the fabrication processes of the flexible and microscale organic memory devices.

Figure 1(f) shows the schematic of the fabricated flexible and microscale organic memory devices. The electrical characteristics of the fabricated flexible organic memory devices were measured with a semiconductor parameter analyzer (Keithley 4200 SCS) and a probe station system (JANIS Model ST-500) in vacuum condition. The flexible condition was accomplished by attaching samples on the surface of a semicylindrical plastic mold.

3. RESULTS AND DISCUSSION

The optical image of the finished 4 K-bit integrated and microscale organic memory devices on a PET substrate is shown in Figure 2(a). In a $1.9 \times 1.9 \text{ mm}^2$ region, 4,096 of micro-sized organic memory cells are integrated with crossbar structure. Figure 2(b) shows the representative current-voltage (I - V) curves of the flexible microscale organic memory devices of PI:PCBM that were acquired under bending configurations with a bending radius (R_{bend}) of 10 mm and 5 mm. The external voltage was applied to the Au top electrode while the Al bottom electrode was grounded. The ON state (that is the low resistance state) and OFF state (that is the high resistance state) were made in the same voltage polarity, which is called “unipolar-type” resistive switching behavior. It has been reported that PI:PCBM composite organic memory devices exhibit rewritable unipolar memory switching.^{13, 17, 19, 22, 29} The particular memory cell (Fig. 2(a)) was turned on at $\sim 4.1 \text{ V}$ and 3.7 V and turned off at $\sim 9.5 \text{ V}$ and 9.3 V in the 10 mm and 5 mm bending conditions, respectively. In both bending conditions, the flexible microscale organic memory device showed similar ON/OFF switching and stable current behaviors in the reading voltage region ($< 0.5 \text{ V}$) with a high ON/OFF ratio ($I_{\text{ON}}/I_{\text{OFF}} \sim 10^5$). The switching mechanism of PI:PCBM composite can be explained by a charge-trapping mechanism, as nano-sized PCBM clusters embedded in PI matrix take the role of charge trapping center.³⁰

Figure 3 shows the distribution of threshold voltages from 20 randomly chosen memory cells in both 10 mm

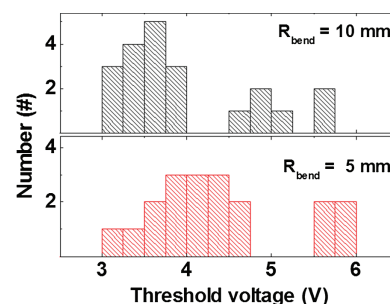


Figure 3. Distribution of the threshold voltage values for the bending radius of 10 mm (upper graph) and 5 mm (lower graph).

and 5 mm bending conditions. In these bending conditions, the threshold voltages were distributed in the range between 3 and 6 V and the mean values of threshold voltages were found to be $\sim 4.0 \text{ V}$ and 4.5 V for 10 mm and 5 mm bending conditions, respectively. The similar threshold voltage distributions among the bending conditions indicate that the individual memory devices can be switched ON uniformly without degradation due to bending conditions.¹⁷

Figure 4(a) shows the ON/OFF current ratios measured at read voltage of 0.3 V from about 20 memory cells for three conditions ($R_{\text{bend}} = \infty$ (flat), 10 mm, and 5 mm). The bending configurations are displayed in the inset of Figure 4(a). We found that the ON/OFF ratio of our flexible microscale organic memory devices maintained about 10^4 and it did not undergo significant electrical degradation under the different bending conditions. We also investigated the memory storage durability. The memory retention test was performed on our flexible memory devices and the results are shown in Figure 4(b). Our flexible and microscale organic memory device exhibited a long retention time up to 10^4 seconds under the bending condition ($R_{\text{bend}} = 5 \text{ mm}$) maintaining very high ON/OFF ratio ($\sim 10^7$) at 0.3 V bias.

All these results suggest that our devices presented good nonvolatile resistive memory behaviors under the various bending configurations. The proper operating microscale

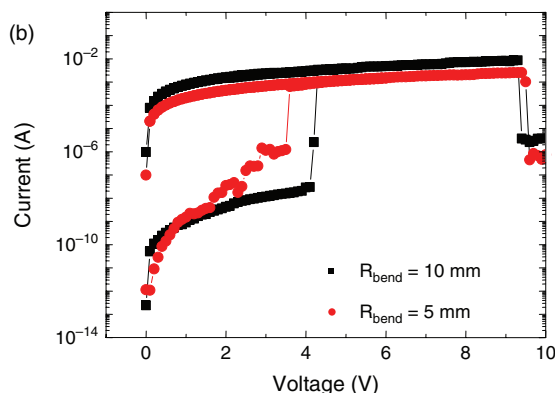
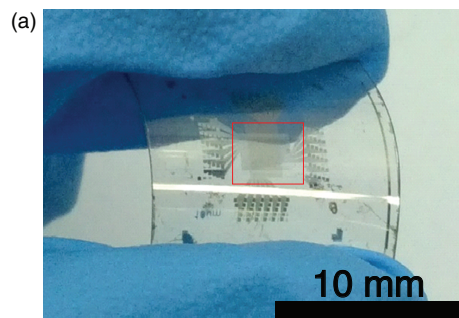


Figure 2. (a) Optical image of fabricated flexible microscale organic memory devices. (b) I - V characteristics of a flexible and microscale organic memory cell measured in bending conditions with a bending radius of 10 mm and 5 mm.

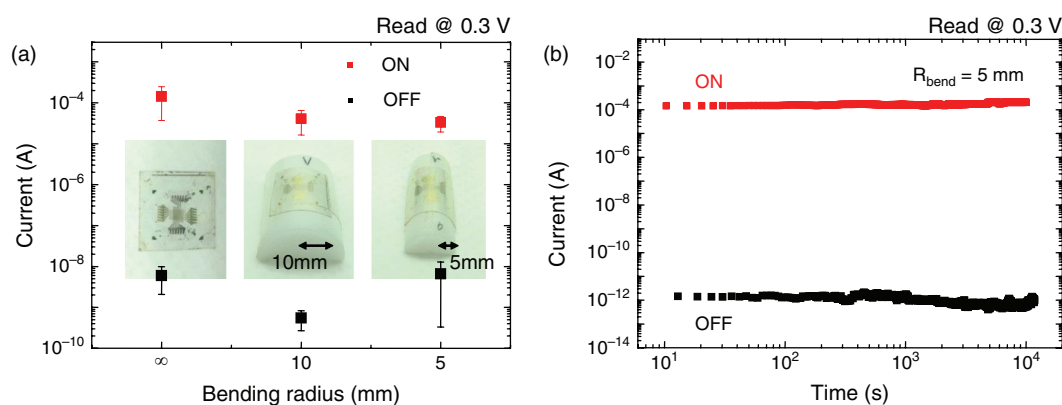


Figure 4. (a) Read current measured at 0.3 V for the ON and OFF states in different bending conditions with a bending radius of ∞ (flat), 10 mm, and 5 mm. (b) Retention time test results for the flexible and microscale organic memory device.

organic memory devices indicate that the orthogonal photolithography method didn't cause serious damage to active organic memory layer, flexible substrate, and electrodes. And the high integration of microscale memory devices was possible due to the large-area processability of photolithographic method. The similarity of electrical characteristics has been also observed in various flexible organic memory devices in macroscale.^{16–21} The similarity for different bending conditions is due to thin active memory layer. The thickness of spin coated PI:PCBM layer is ~ 20 nm. Then the bending strain induced by the length differences between top and bottom layer of PI:PCBM layer would be 4×10^{-6} (film thickness/ R_{bend}) for 5 mm bending radius, which is very small so that interval between nanoscale PCBM clusters is almost not changed with bending conditions. Therefore with ignorable deformation, the active film can function uniformly under mild bending conditions.

4. CONCLUSIONS

We demonstrated the integration of flexible and microscale organic nonvolatile resistive memory devices fabricated as a 64×64 (4,096 cells in 1.9×1.9 mm² area) cross-bar array structure on a plastic substrate. An orthogonal photolithography method with fluorinated photoresist and solvents was used to fabricate the flexible and microscale organic memory devices without causing damage to the underlying organic memory materials. Our flexible and microscale organic memory devices exhibited good ON/OFF ratio ($I_{\text{ON}}/I_{\text{OFF}} < 10^4$) under bending conditions (bending radius of 10 mm and 5 mm). The devices also showed good retention performance as they maintained for 10,000 seconds without any serious degradation.

Acknowledgments: This work was accomplished through support from the National Creative Research Laboratory Program (grant No. 2012026372) provided by the National Research Foundation of Korea (NRF) grant funded by the Korean Ministry of Science, ICT and Future

Planning. Seunghun Hong acknowledges the support from the NRF grant (H-GUARD 2013M3A6B2078961) and Jin-Kyun Lee thanks the financial support from the Fundamental R&D Program for Core Technology of Materials (grant No. 10041220) funded by the Korean Ministry of Knowledge Economy.

References and Notes

1. J. Heeger, S. Kivelson, J. R. Schrieffer, and W. P. Su, *Rev. Mod. Phys.* 60, 781 (1988).
2. S. R. Forrest, *Nature* 428, 911 (2004).
3. M. Muccini, *Nat. Mater.* 5, 605 (2006).
4. L. Briseno, S. C. B. Mannsfeld, M. M. Ling, S. Liu, R. J. Tseng, C. Reese, M. E. Roberts, Y. Yang, F. Wudl, and Z. Bao, *Nature* 444, 913 (2006).
5. H. Yan, Z. Chen, Y. Zheng, C. Newman, J. R. Quinn, F. Dotz, M. Kastler, and A. Facchetti, *Nature* 457, 679 (2009).
6. T. Sekitani, H. Nakajima, H. Maeda, T. Fukushima, T. Aida, K. Hat, and T. Someya, *Nat. Mater.* 8, 494 (2009).
7. M. Segal, M. Singh, K. Rivoire, S. Difley, T. V. Voorhis, and M. A. Baldo, *Nat. Mater.* 6, 374 (2007).
8. H. Schwartz, B. C. Tee, J. Mei, A. L. Appleton, H. Kim Do, H. Wang, and Z. Bao, *Nat. Commun.* 4, 1859 (2013).
9. J. Ouyang, C. W. Chu, C. R. Szmanda, L. Ma, and Y. Yang, *Nat. Mater.* 3, 918 (2004).
10. Y. Yang, J. Ouyang, L. Ma, R. J.-H. Tseng, and C.-W. Chu, *Adv. Funct. Mater.* 16, 1001 (2006).
11. J. C. Scott and L. D. Bozano, *Adv. Mater.* 19, 1452 (2007).
12. Q.-D. Ling, D.-J. Liaw, C. Zhu, D. S.-H. Chan, E.-T. Kang, and K.-G. Neoh, *Prog. Polym. Sci.* 33, 917 (2008).
13. B. Cho, S. Song, Y. Ji, T.-W. Kim, and T. Lee, *Adv. Funct. Mater.* 21, 2806 (2011).
14. Y. Ji, B. Cho, S. Song, M. Choe, T.-W. Kim, J.-S. Kim, B.-S. Choi, and T. Lee, *J. Nanosci. Nanotechnol.* 11, 1385 (2011).
15. S. Song, T.-W. Kim, B. Cho, Y. Ji, and T. Lee, *J. Nanosci. Nanotechnol.* 11, 4492 (2011).
16. Y. Ji, D. F. Zeigler, D. S. Lee, H. Choi, A. K.-Y. Jen, H. C. Ko, and T.-W. Kim, *Nat. Commun.* 4, 2707 (2013).
17. S. Song, J. Jang, Y. Ji, S. Park, T.-W. Kim, Y. Song, M.-H. Yoon, H. C. Ko, G.-Y. Jung, and T. Lee, *Org. Electron.* 14, 2087 (2013).
18. D. Y. Yun, W. S. Song, T. W. Kim, S. W. Kim, and S. W. Kim, *Appl. Phys. Lett.* 101, 103305 (2012).
19. Y. Ji, B. Cho, S. Song, T.-W. Kim, M. Choe, Y. H. Kahng, and T. Lee, *Adv. Mater.* 22, 3071 (2010).
20. Y. Ji, S. Lee, B. Cho, S. Song, and T. Lee, *ACS Nano* 5, 5995 (2011).

21. D.-I. Son, J.-H. Kim, D.-H. Park, W. K. Choi, F. Li, J. H. Ham, and T. W. Kim, *Nanotechnology* 19, 055204 (2008).
22. J. J. Kim, B. Cho, K. S. Kim, T. Lee, and G. Y. Jung, *Adv. Mater.* 23, 2104 (2011).
23. J. E. Green, J. W. Choi, A. Boukai, Y. Bunimovich, E. Johnston-Halperin, E. DeIonno, Y. Luo, B. A. Sheriff, K. Xu, Y. S. Shin, H.-R. Tseng, J. F. Stoddart, and J. R. Heath, *Nature* 445, 414 (2007).
24. K. W. Lek, R. J. Tseng, W. Wei, P. Qibing, and Y. Yang, *Presented at Proc. IEEE int. Electron Device Meeting* (2007), p. 12.
25. A. Zakhidov, J.-K. Lee, H. H. Fong, J. A. DeFranco, M. Chatzichristidi, P. G. Taylor, C. K. Ober, and G. G. Malliaras, *Adv. Mater.* 20, 3481 (2008).
26. J.-K. Lee, M. Chatzichristidi, A. A. Zakhidov, P. G. Taylor, J. A. DeFranco, H. S. Hwang, H. H. Fong, A. B. Holmes, G. G. Malliaras, and C. K. Ober, *J. Am. Chem. Soc.* 130, 11564 (2008).
27. A. Zakhidov, J.-K. Lee, J. A. DeFranco, H. H. Fong, P. G. Taylor, M. Chatzichristidi, C. K. Ober, and G. G. Malliaras, *Chem. Sci.* 2, 1178 (2011).
28. Y. Ouyang, J.-K. Lee, M. E. Krysak, J. Sha, and C. K. Ober, *J. Mater. Chem.* 22, 5746 (2012).
29. Y. Song, J. Jang, D. Yoo, S.-H. Jung, S. Hong, J.-K. Lee, and T. Lee, *Org. Electron.* 17, 192 (2014).
30. L. D. Bozano, B. W. Kean, V. R. Deline, J. R. Salem, and J. C. Scott, *Appl. Phys. Lett.* 84, 607 (2004).

Received: 12 January 2014. Accepted: 16 March 2015.

Delivered by Ingenta to: Seoul National University
IP: 147.47.51.103 On: Mon, 18 Jul 2016 02:47:01
Copyright: American Scientific Publishers